Received: 16 March 2022 | Revised: 25 August 2022 | Accepted: 27 August 2022

DOI: 10.1002/hyp.14686

RESEARCH ARTICLE

WILEY

Spatial and temporal dynamics of water isotopes in the riverine-marine mixing zone along the German Baltic Sea coast

Bernhard Aichner[1] | Timo Rittweg[2] | Rhena Schumann[3] | Sven Dahlke[4] | Svend Duggen[5] | David Dubbert[6]

[1]Department of Community and Ecosystem Ecology, Leibniz Institute of Freshwater Ecology and Inland Fisheries, Berlin, Germany

[2]Department of Fish Biology, Fisheries and Aquaculture, Leibniz Institute of Freshwater Ecology and Inland Fisheries, Berlin, Germany

[3]Biological Station Zingst, University of Rostock, Zingst, Germany

[4]Biological Station Hiddensee, University of Greifswald, Kloster, Germany

[5]A. P. Møller Skolen, Schleswig, Germany

[6]Department of Ecohydrology and Biogeochemistry, Leibniz Institute of Freshwater Ecology and Inland Fisheries, Berlin, Germany

Correspondence
Bernhard Aichner, Department of Community and Ecosystem Ecology, Leibniz Institute of Freshwater Ecology and Inland Fisheries, Müggelseedamm 301, Berlin D-12587, Germany.
Email: bernhard.aichner@gmx.de

Funding information
Deutsche Forschungsgemeinschaft

Abstract

River estuaries are characterized by mixing processes between freshwater discharge and marine water masses. Since the first are depleted in heavier stable isotopes compared with the marine realm, estuaries often show a linear correlation between salinity and water stable isotopes ($\delta^{18}O$ and $\delta^{2}H$ values). In this study, we evaluated spatial and seasonal isotope dynamics along three estuarine lagoon transects, located at the northern German Baltic Sea coast. The data show strong seasonality of isotope values, even at locations located furthest from the river mouths. They further reveal a positive and linear salinity-isotope correlation in spring, but -in two of the three studied transects- hyperbolic and partially reverse correlations in summers. We conclude that additional hydrological processes partially overprint the two-phase mixing correlation during summers: aside from the isotope seasonality of the riverine inflows, the shallow inner lagoons in the studied estuaries are influenced by evaporation processes. In contrast the estuarine outflow regions are under impact of significant salinity and isotope fluctuations of the Baltic Sea. Deciphering those processes is crucial for the understanding of water isotope and salinity dynamics. This is also of relevance in context of ecological studies, for example, when interpreting oxygen and hydrogen isotope data in aquatic organisms that depend on ambient estuarine waters.

KEYWORDS
$\delta^{2}H$, $\delta^{18}O$, Baltic Sea, bodden, Rügen, salinity, Schlei, Zingst

1 | INTRODUCTION

The water cycle, or hydrological cycle, refers to the movement of water molecules throughout the globes geological, biological and ecological compartments. Major constituents of this cycle are water evaporating from the oceans, transportation of vapour to continental realms, re-condensation to rain droplets, and back flow via groundwater and surface flow towards the ocean. The varying physical properties, specifically the different weights of stable oxygen and hydrogen isotopes of the water molecule (^{16}O, ^{17}O, ^{18}O, ^{1}H, ^{2}H), lead to isotope fractionation during all these processes (Craig, 1961; Dansgaard, 1964). As a consequence, the isotopic signature of water in both the liquid and the vapour phase is characterized by spatial and temporal variability, and in principal is depleted of the heavier isotopes in water vapour and

continental freshwater, compared with the ocean water (Gat & Gonfiantini, 1981). For this reason, mixing processes in the transitional zone between the riverine/freshwater and marine/saline realm lead to linear relationships between salinity and water isotopes, as observed in multiple river estuaries around the globe (Barrie et al., 2015; Chamberlayne et al., 2021; Ingram et al., 1996; Mohan & Walther, 2015; Price et al., 2012; Swart & Price, 2002).

In precipitation, isotopes exhibit a seasonal signal, with lower/higher values in the cold/warm season, respectively (Bowen & Revenaugh, 2003). Riverine and lacustrine systems reflect this signal (Dutton et al., 2005; Ogrinc et al., 2008; Halder et al., 2015; Orlowski et al., 2016; Reckerth et al., 2017; Aichner et al., 2021), but the seasonal amplitude is attenuated and timing of the signal delayed by 1–3 months (Bittar et al., 2016; Jasechko et al., 2016; Reckerth et al., 2017; Rodgers et al., 2005). The reasons for the time delay between precipitation and river/lake water isotopes, and the smaller seasonal amplitude of the latter, can be attributed to multiple catchment characteristics and processes. Crucial influencing factors on how fast a precipitation isotope signal is transferred into fluvial systems are the flow regime of rivers, and the area, topography and geology of their catchments (Maloszewski et al., 1992; McGuire et al., 2005; Rodgers et al., 2005; Sklash et al., 1976).

In water bodies with high residence time of the water, such as large and/or voluminous lakes or in the marine realm, the seasonal $\delta^{18}O$ and $\delta^{2}H$ variability decreases. Instead, mixing processes of water from different sources with variable isotopic signatures, become more dominant on the actual isotopic signature (Benetti et al., 2017; Craig & Gordon, 1965; Frew et al., 2000). The North Sea, for example, is influenced by both North Atlantic water with high salinity, entering the North Sea basin from the northeast, and inflow of brackish water and freshwater, derived from the Baltic Sea and from rivers, respectively (Harwood et al., 2008). The Baltic Sea, in turn experiences occasional inflow intrusion from the North Sea (higher $\delta^{18}O$ and $\delta^{2}H$ values), but also constantly receives freshwater discharge from rivers (lower δ-values). For these reasons, water isotopes show a strong positive correlation with salinity in both the Baltic Sea and North Sea (Ehhalt, 1969; Frohlich et al., 1988; Jefanova et al., 2020; Richter & Kowski, 1990; Torniainen et al., 2017).

Isotope signatures of the ambient water are mirrored in the local fauna and flora. For example, fish incorporate elements from ambient water into their body structures, (Zanden et al., 2016). These structures form through precipitation from the water the fish currently lives in, and as such mirror the current isotopic profile of the water (Patterson et al., 1993). In recent years, oxygen isotopic ratios of ear bones (otoliths) have been commonly used in studies of migration and geolocation of fish, for example to develop isoscapes, that is predictive surfaces of large-scale water isotope data. Those were used to retrospectively predict the whereabouts of migrating fish (Brennan et al., 2019; Torniainen et al., 2017; Trueman et al., 2012), and to assign fish to discrete, geographically segregated stocks (Matta et al., 2010). With respect to aquatic plants or algae, their cellular lipid compounds have been shown to track the hydrogen isotopic signature of the ambient water, but with a potential additional influence of varying salinity (Aichner et al., 2017; Häggi et al., 2015; He et al., 2020; Ladd & Sachs, 2015, 2017; Sachs & Schwab, 2011; Schouten et al., 2006). These dependencies have frequently been applied in paleoclimatic studies, for reconstruction of past hydrological conditions and salinities (e.g. Aichner et al., 2019; Leduc et al., 2011; Meer et al., 2007).

Knowledge and understanding about water isotopic gradients and the hydrological processes behind, has great potential to facilitate application and interpretation of oxygen and hydrogen isotopic compositions in biogenic carbonates and plant lipids. In this study, we analysed water isotope dynamics in estuarine river and lagoon systems along the northern German Baltic Sea coast. Main questions were: (1) how far are seasonal isotope signals in rivers transmitted into Baltic Sea estuarine systems? (2) what are the major processes behind the observed gradients? (3) are water isotopes a predictor for salinity in the riverine-marine mixing zone? The major aim was to understand how hydrological processes control seasonal and spatial water isotope variability in this study area.

2 | STUDY AREA

The northeastern German coast of the Baltic Sea is basically a flooded glacial moraine landscape. It is characterized by extensive bays, shallow lagoons (the boddens) and marine inlets, which form the mixing zone between rivers and the marine realm (Correns, 1977; Schwarzer et al., 2008). These zones are characterized by hydrologic events which in turn affect biochemical characteristics of the ecosystem. For example they react sensitively both to discharge pulses from rivers and inflow events from the marine side after storms (Gocke et al., 2003). Furthermore, a dense net of water management structures, such as water retention flaps, partially attenuate freshwater flow from creeks into the lagoons. Here, automatic ones will release water from creeks when the lagoons are low while some manual flaps exist, which are operated by hand (Funkel, 2004) .

For this study, water samples were taken along three transects, encompassing salinity gradients (Figures 1 and 2; Tables S1 and S2):

a. The Schlei estuary (Figures 1 and 2a) is a flooded sub-glacial channel, extending ca. 42 km from the major Baltic Sea coast line towards the inlands. The inner Schlei comprises the two larger basins of the 'Kleine Breite' and 'Große Breite', while the outer Schlei at some sections resembles a wider river. Adjacent, several 'noors', that is water bodies similar to lakes, are connected to the main Schlei often by just narrow outlets. The Schlei has one medium sized inflow, the Füsinger Au at Kleine Breite, and several small creeks entering along the whole length of the water body. The salinity gradient is linearly increasing from 0 to 3 psu at the inner Schlei (Burgsee and Kleine Breite) towards values of ca. 15–20 psu near the outflow to the Baltic Sea (Gocke et al., 2003; Grupe et al., 2009; LLUR, 2001; Seiß, 2014). This gradient is seasonally influenced by relatively high freshwater discharge in winter and spring compared with summers. In addition, episodic sea level changes by ±0.5–1.5 m, caused by strong winds, lead to rapid movement of water masses within the Schlei, which superimposes the salinity gradient (Schulz, 1979). Saltwater intrusion events,

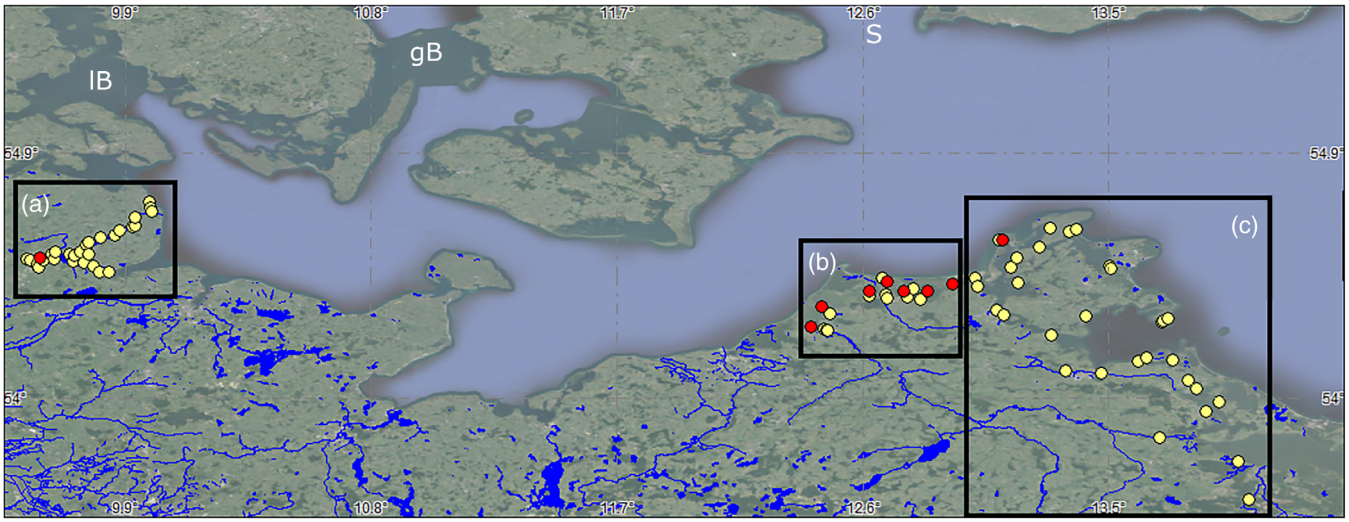

FIGURE 1 Transect sample points at (a) Schlei, (b) Darss-Zingst Bodden chain (DZBC) and (c) East Transect (Stettiner Haff—Peenestream—Greifswalder Bodden—Rügener Boddens). Red circles: Time series sampling March 2020–March 2021. Yellow circles: Seasonal sampling (June 2019, March 2020, July 2020). gB, Great Belt; lB, Little Belt; S, Øresund. Sampling points are listed in Tables S1 and S2.

from the North Sea into the Baltic Sea (Mohrholz, 2018a, 2018b) (Figure 3) similarly have the potential to increase salinity values in the outer Schlei, as visible for March 2020 in contrast to July 2020 (Figure 2a).

b. The Darss-Zingst Bodden chain (DZBC) is a system of several shallow water basins, which mostly do not exceed 2–3 m water depth (Figures 1 and 2b). The rivers Recknitz and Barthe are major inflows and there are two outflows towards the Baltic Sea, which lie close to each other at the easternmost end of the Darss-Zingst peninsula. The salinity gradient is covering the range from almost freshwater conditions near the Recknitz and Barthe inflows to ca. 10 psu near the outflows (Chubarenko et al., 2005). The latter reflect the salinity levels of the adjacent Baltic Sea, which are lower than in the more western Baltic realms (where the Schlei is situated), but likewise influenced by salt water intrusion events (Figure 2b). The DZBC can be divided into an inner/western part (Saaler Bodden and Bodstedter Bodden), which is mainly influenced by riverine inflows, and an outer/eastern part (Barther Bodden and Grabow), which is more susceptible to Baltic water inflow during conditions of east winds (Schumann et al., 2006). The two parts are connected by the Zingster Stream (ZS), a narrow and deep water channel located in the central bodden chain.

c. the easternmost transect reaches from the Stettiner Haff, via the Greifswalder Bodden to the multiple lagoons which form the western and northern bodden chains around the isle Rügen (WRBC and NRBC) (Figures 1 and 2c). While the covered salinity gradient is similar than in the DZBC (i.e. 0 – ca. 10 psu), several inflows and connections to the Baltic Sea create a highly dynamic system in pronounced exchange with marine water (Bachor, 2005; Correns & Jäger, 1979; Hübel et al., 1998; Hübel & Dahlke, 1999). The Stettiner Haff is strongly under influence of the Oder river, which contributes >95% of the riverine discharge along the northeastern German Baltic Sea coastline (Richter & Kowski, 1990). Salinity is gradually increasing between the Stettiner Haff, along the Peenestream towards the Greifswalder bodden (Figure 2c) (Lampe, 1999). The latter is a larger basin of max 13.5 m depth which is separated to the open Baltic Sea by the 'Greifswalder Boddenrandschwelle', a glacial terminal moraine which builds a just 1–2.5 m deep shallow. The Greifswalder Bodden is connected by the Strela Sound to the WRBC, which in turn terminates in the Vitter Bodden next to Hiddensee island. The same bodden can be seen as terminal basin of the inner or northern Rügen bodden chain (NRBC; reaching from Kleiner Jasmunder Bodden via Großer Jasmunder, Breeger and Wieker Bodden), which is characterized by a salinity gradient from 0 to ca. 10 psu, comparable as in the DZBC (Birr, 1997; Schiewer, 2008).

3 | MATERIAL AND METHODS

3.1 | Water sampling

Water samples were taken along transects (yellow dots in Figure 1) in June 2019 (lower spatial density of sampling points), March 2020 and July 2020. They were collected close to shores with a pipette from ca. 40 to 60 cm below water surface and directly transferred into a measurement vial. The vials were instantly closed and stored in a cooling box, before being placed in a fridge until further processing.

At selected spots, time series were sampled every 2–4 weeks (A: Schlei, A. P. Møller Skolen Schleswig; E: Zingster Stream, Biological Station; I: Vitter Bodden, Kloster/Hiddensee) or monthly (B–D, F–G: Zingster Bodden) from March 2020 to March 2021. Samples from A and I were taken accordingly to shore samples, while samples B–H were taken in deep parts of the boddens, close to buoys marking long-term monitoring locations. For the latter, a Limnos water sampler was used to obtain 2 l samples from 0.5 to 1.0 m depth below water surface, of which 1.5 ml were transferred into measurement vials.

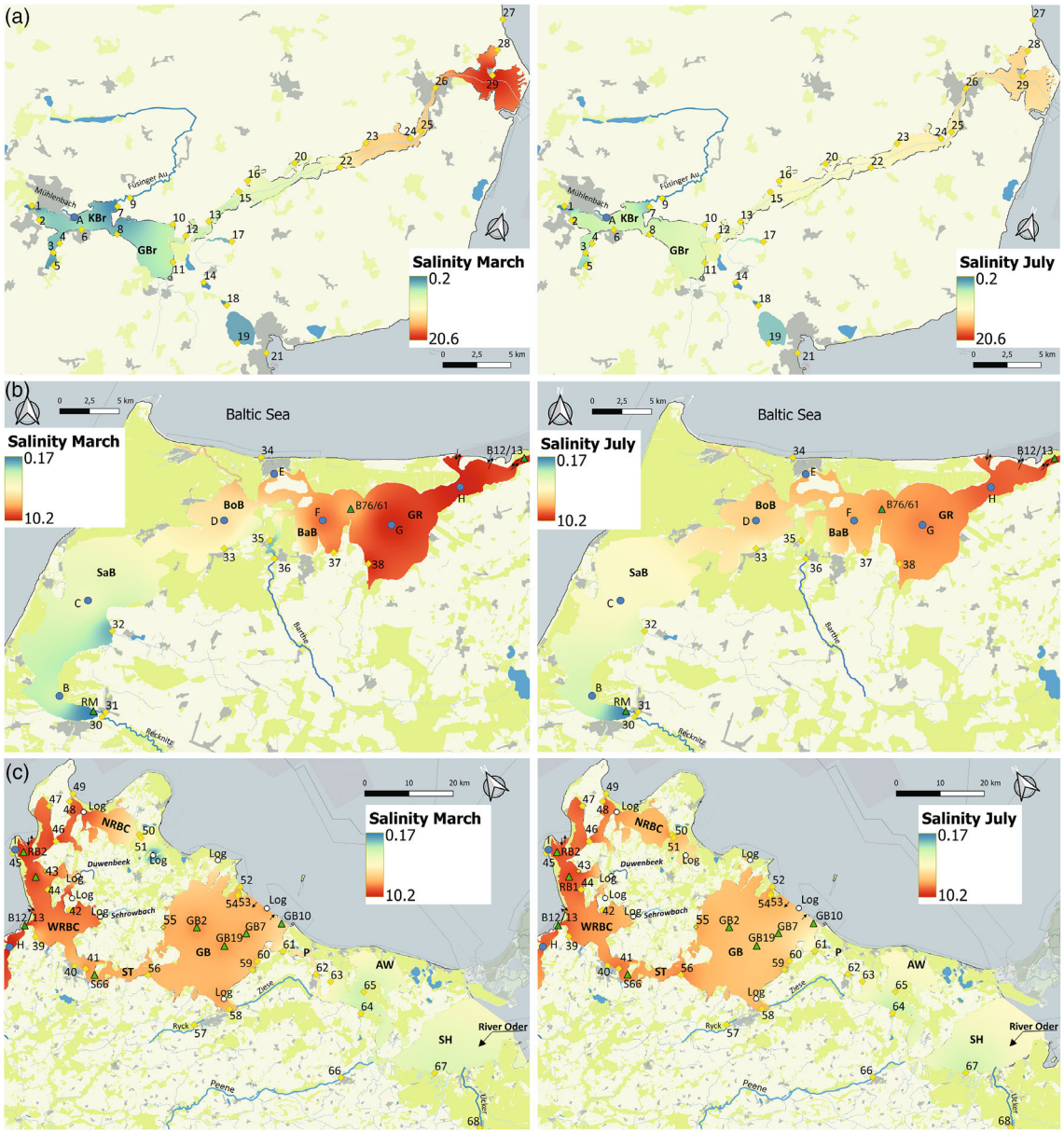

FIGURE 2 Salinity in March (left) and July (right) 2020 in (a) the Schlei; (b) the DZBC; and (c) the East Transect. Panels a–c refer to sub-regions as indicated in Figure 1. Different colour scales are due to different salinity gradients in these sub-regions. Blue circles #A–I: Sampling points for time series. Yellow circles #1–68: Shore samples. Green triangles indicate long-term monitoring points from local authorities, and white circles ('Log') spots with installed salinity loggers, both delivering data included into salinity interpolation. Double arrows indicate exchange points with Baltic Sea water. AW, Achterwasser; BaB, Barther Bodden; BoB, Bodstedter Bodden; GB, Greifswalder Bodden; GBr, Große Breite; GR, Grabow; KBr, Kleine Breite; NRBC, Northern Rügen Bodden chain; P, Peenestream; SaB, Saaler Bodden; SH, Stettiner Haff; ST, Strela sound; WRBC, Western Rügen Bodden chain.

3.2 | Water chemical parameters

Water chemical parameters were measured in situ at shore transect and time series sampling spots A and I, using a Multi 3630 IDS multi-parameter device (WTW, Weilheim, Germany), equipped with a WTW TetraCon 925 electrical conductivity measuring cell. At the A. P. Møller Skolen, salinity and temperature were measured using a modular multi-parameter probe (WTW multimeter 3440), mounted with TetraCon® 925-P and MPP 930 IDS electrical conductivity cells. Before each application the cells were calibrated with E-Set Trace 0.01 M KCl calibration solution based on PTB/NIST. For samples from DZBC-timeseries (spots B–H), a WTW 1970i conductivity meter and TetraCon 325 measuring cell were used to analyse electrical conductivity/salinity in the laboratory.

Salinity maps (Figure 2) were produced in QGIS 3.14, using the inverse distance weighted interpolation tool with a squared weighting coefficient, for the sampling periods March and July 2020. Herefore, the in situ measured salinity values were used for spatial interpolation,

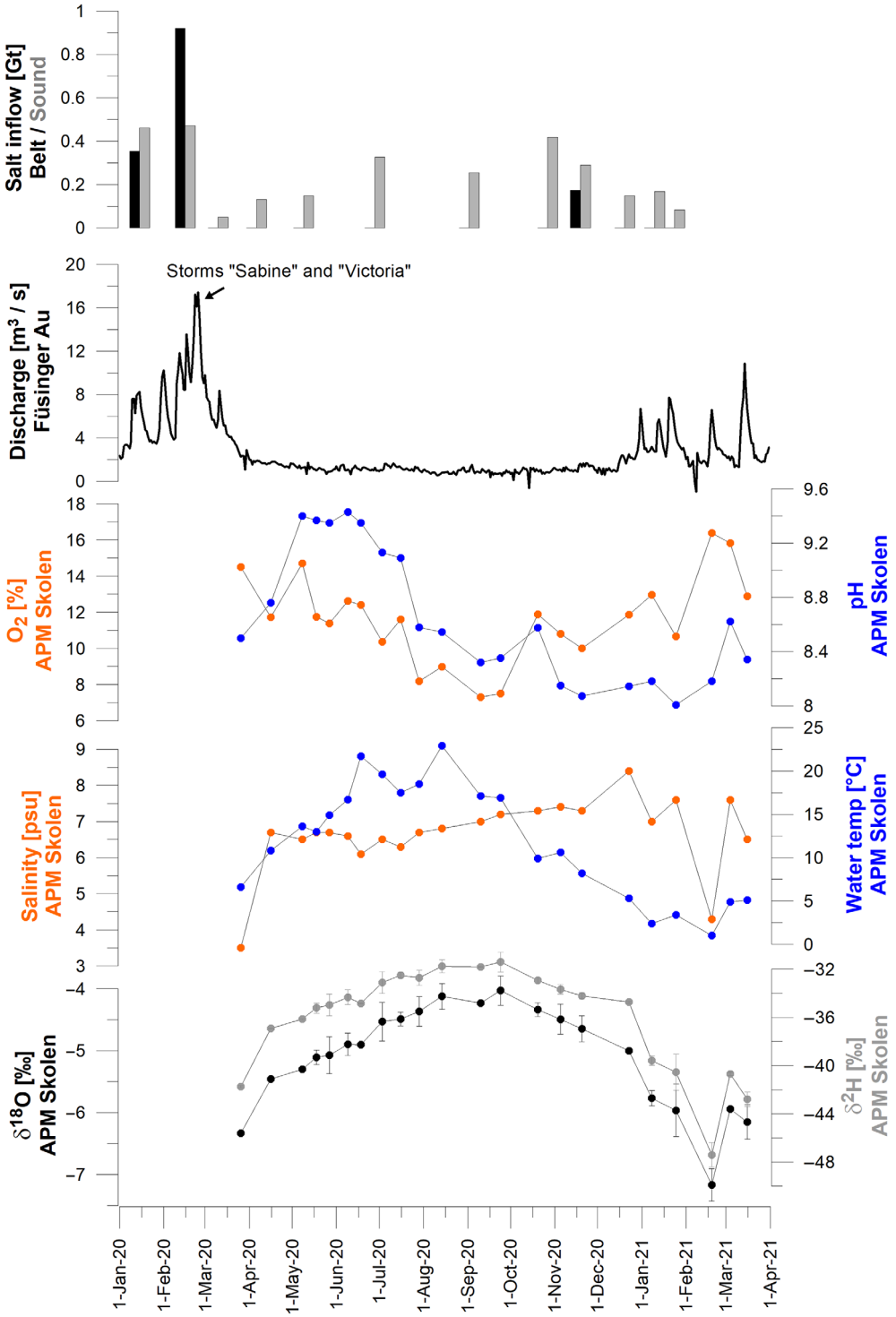

FIGURE 3 Time series of $\delta^2H/\delta^{18}O$ values in water samples collected between 26th March 2020 and 16th March 2021 near A. P. Møller Skolen (APM Skolen), Schleswig (Kleine Breite, Schlei; sampling point #A; Figure 2a). Error bars indicate standard deviation of replicate measurements. Salinity, water temperature, O_2-concentration and pH measured in situ during sampling. Data of daily mean values of water discharge derived from the major inflowing river Füsinger Au (LLUR, 2022). Major Baltic Sea salt inflow events at Great Belt and Øresund from (Mohrholz, 2018a, 2018b).

in combination with data derived from monthly monitoring stations of local authorities (LUNG; Landesamt für Umwelt, Naturschutz, Geologie of the German State Mecklenburg-Vorpommern) (Figure 2). Some additional values were derived from HOBO U24-002-C salinity loggers (Onset, Bourne, USA), which were installed at different locations around the Rügener Boddens. Data were only interpolated within the riverine-marine mixing zone, while the open Baltic Sea was excluded.

3.3 | Isotope measurement

Water samples were filtered (0.2 µm cellulose acetate) prior to analysis of stable isotopes ($\delta^{18}O$ and δ^2H values) in the water isotope lab at IGB Berlin, using a Picarro (Santa Clara, CA, USA) L2130-i cavity ring-down spectrometer. Measurements were routinely checked for organic contamination using the Picarro ChemCorrect software.

Isotope values and standard deviations are based on six replicate measurements of each sample, discarding the first three measurements to account for memory effects. In house criteria excluded all injections with a water SD higher than 400 ppm or water amount deviation greater than 3000 ppm to furthermore improve precision.

For instrument calibration we used three laboratory standards for each group of 24 samples: L ($\delta^{18}O$ −17.86 ‰ and $\delta^{2}H$ −109.91 ‰), DEL ($\delta^{18}O$ −10.03 ‰ and $\delta^{2}H$ −72.81 ‰), H ($\delta^{18}O$ 2.95 ‰ and $\delta^{2}H$ 0.29 ‰). A fourth lab standard, M ($\delta^{18}O$ −7.68 ‰ and $\delta^{2}H$ −56.70 ‰), was used as quality and drift control after every six samples. All lab standards were referenced against primary measurement standards: VSMOW2 (Vienna Standard Mean Ocean Water 2), GRESP (Greenland Summit Precipitation) and SLAP2 (Standard Light Antarctic Precipitation 2) from the IAEA (International Atomic Energy Agency, Vienna, Austria).

The measurement uncertainty was quantified by error propagation, including the parameters: (a) uncertainties of lab standards; (b) errors of standard calibration; (c) average standard deviation of replicate measurements. Based on this, measurement uncertainty was estimated to account 0.16 ‰ for $\delta^{18}O$ and 0.57 ‰ for $\delta^{2}H$.

4 | RESULTS

4.1 | Time series

Water samples collected at the A. P. Møller Skolen (Kleine Breite, Schlei; sampling point #A), Biological Station Zingst (ZS, #E) and Hiddensee/Kloster (Vitter Bodden; #I) all exhibit clear seasonal isotopic trends (Figures 3–6). The seasonal amplitude is in range of ca. 10–15

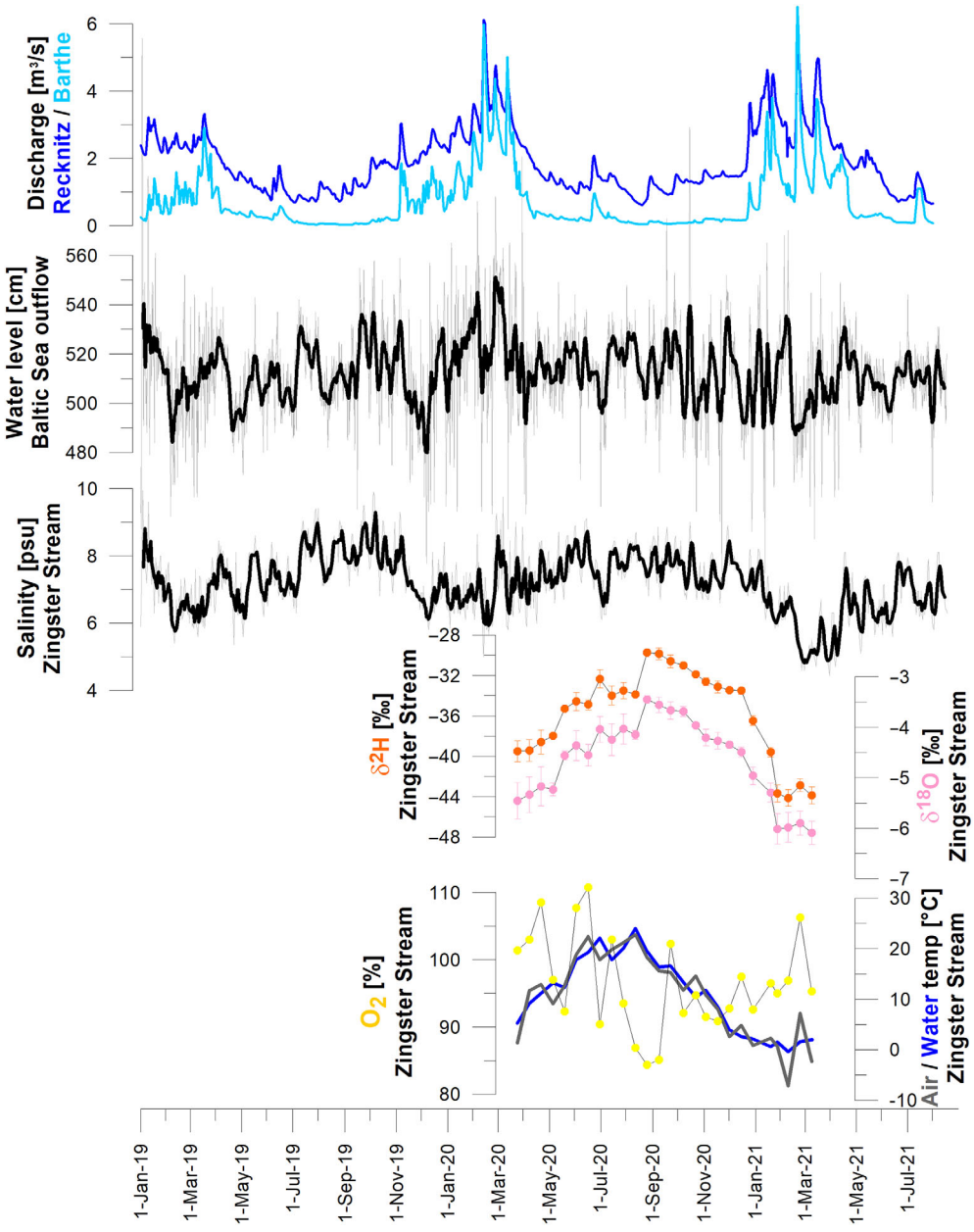

FIGURE 4 Time series of $\delta^{2}H/\delta^{18}O$ values in water samples collected between 24th March 2020 and 9th March 2021 at Biological Station Zingst (Zingster Stream; sampling point #E; Figure 2b). Error bars: Standard deviation of replicate measurements. Water temperature and salinity derived from long-term daily monitoring program conducted at Biol. Station Zingst. Water levels at the bodden outflow towards the Baltic Sea near Barhöft provided by WSA-WSV (2022): Thick black line indicates 5-point average. Riverine discharge of Recknitz and Barthe from STALU (2022).

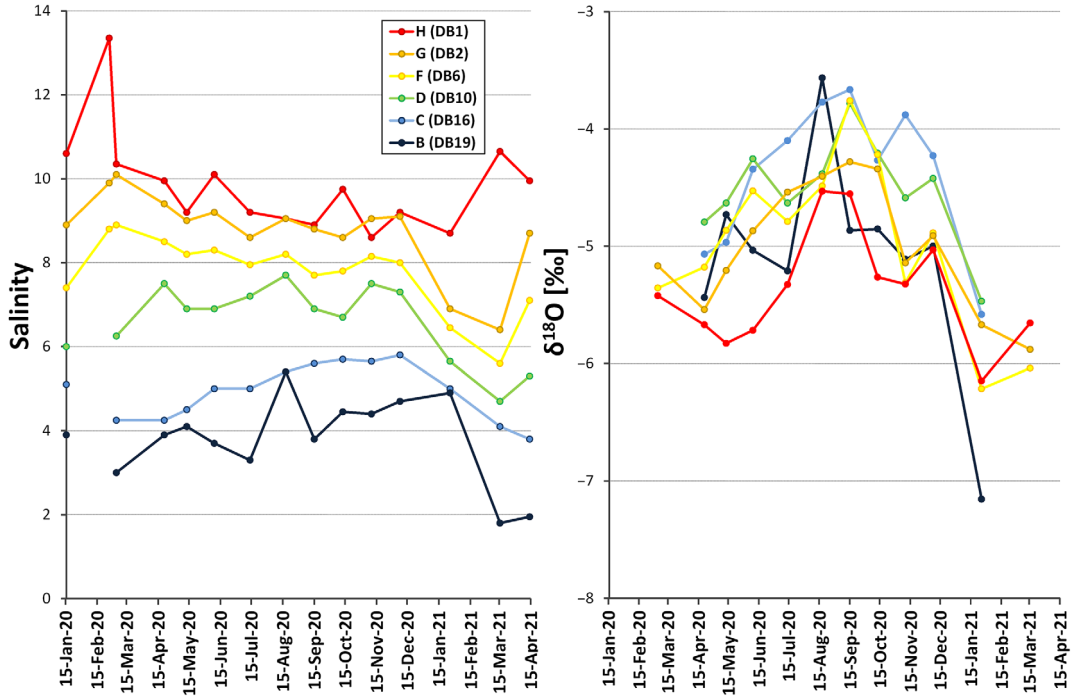

FIGURE 5 Time series of (a) salinity and (b) $\delta^{18}O$ values in water samples collected monthly at a transect along the Zingster Bodden chain. Sample points reaching from buoys located near the inflow of the river Recknitz (sampling spot #B; LUNG monitoring point DB19) to those located close to the outflow towards the Baltic Sea (sampling spot H; LUNG monitoring point DB 1).

‰ (δ^2H) and 2–2.5 ‰ ($\delta^{18}O$), reaching minimum and maximum values in February/March and September/October, respectively.

In contrast to water isotope values, the salinities showed variable trends at the different sampling locations. At the Schlei (point #A), values were relatively constant (ca. 6–7 psu) at most measuring days within the sampling period (26th March 2020 to 16th March 2021) (Figure 3). Exceptions were two samples from 26th March 2020 and 19th February 2021, which showed decreased salinity values of 3.5–4.3 psu. Those are mirrored by lower δ-values in water samples collected at those 2 days.

In the DZBC (sampling points #B–H), the salinity values exhibited pronounced seasonal trends throughout the studied time period (24th March 2020 to 9th March 2021) (Figures 4 and 5). At the ZS (point #E), they show lower values in winter/spring and higher values in summers, hence they resemble the seasonal water isotope trend (Figure 4). This is also true for the sampling spots in the western part of the DZBC (#B, #C, #D), that is close to the inflow of the river Recknitz. In the eastern part (#F, #G, #H), this seasonality becomes less pronounced (Figure 5). Close to the outflow towards the Baltic Sea (point #H), peak salinities up to 14 psu were observed in February 2020 and March 2021.

At Vitter Bodden (Hiddensee/Kloster; sampling point #I), the salinity measurements showed values around 9–10 psu, with a slight decreasing tendency throughout the sampling period (18th March 2020 to 3rd March 2021) (Figure 6). Maximum values up to 11.2 psu were observed in late winters 2020 and 2021. Hence, the seasonal trend in the Vitter Bodden resembles the conditions at the outflow of the DZBC (point H).

4.2 | Transects

Similar to salinity gradients (Figure 2), the water isotope values in March 2020 increase from low to high along all three transects, that is from river inlets to the outflows to the Baltic Sea (exemplarily plotted for $\delta^{18}O$ values in Figure 7). In July 2020, most regions show higher δ-values compared with March (Figure 7; interpolated maps with isotope offsets between the two seasons in Figure S1). Especially, the innermost waterbodies, such as Kleine and Große Breite (Schlei), the Saaler Bodden (DZBC) and the NRBC, exhibit relatively strong increases of isotope values (Figures 7 and S1). Exceptions from these trends are areas under direct influence of Baltic Sea water, such as the outflow regions of the Schlei and DZBC, which show lower δ-values in July compared with March (Figure 7).

These dependencies lead to isotope gradients which are much less pronounced in July 2020, compared with March. Specifically, the DZBC shows almost homogenous isotope values along the whole bodden chain in July 2020, with exception of the areas directly adjacent to river inflows (Figure 7b). In the following, isotope-salinity correlations are closer examined.

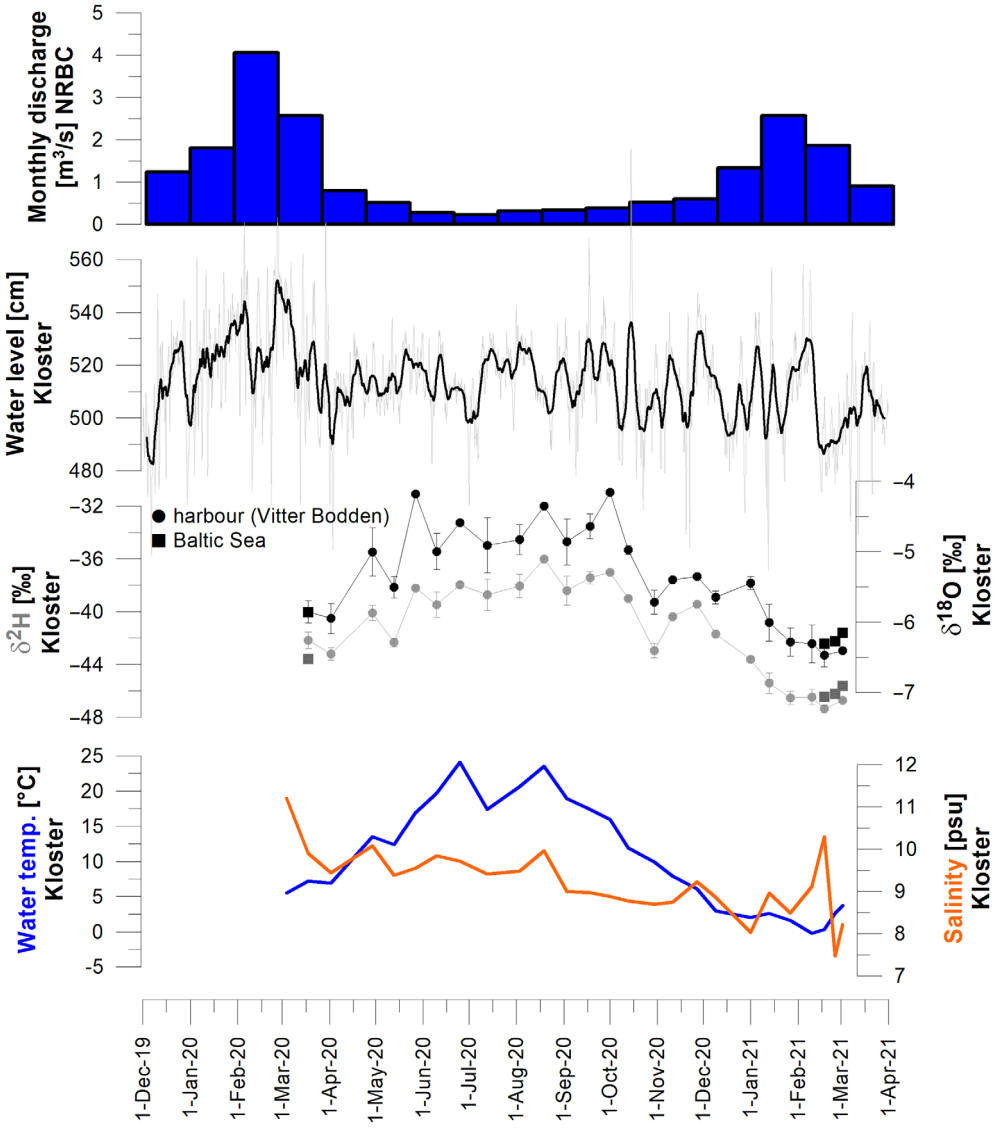

FIGURE 6 Time series of $\delta^2H/\delta^{18}O$ values in water samples collected between 18th March 2020 and 3rd March 2021 at the ferry harbour Kloster, Hiddensee (Vitter Bodden; sampling point #I), in comparison to salinity and water temperature. Error bars indicate standard deviation of replicate isotope measurements. Water levels from Kloster provided by WSA-WSV (2022). Monthly surface flow data from NRBC to Vitter Bodden from STALU (2022).

5 | DISCUSSION

5.1 | Surface runoff and Baltic Sea dynamics drive estuarine salinity

The salinity in Baltic Sea estuarine lagoons is strongly influenced by the seasonal discharge patterns of the inflowing rivers, which in turn is characterized by maximum runoff in the late winter and in spring (Cyberski et al., 2000). During our sampling period, especially the major winter storms 'Sabine' and 'Victoria', lead to increased precipitation and consequently higher surface runoff of rivers and creeks in February 2020 (Figures 3, 4 and 6).

The sampling spot #A is located about 5 km west of the mouth of the Füsinger Au. This river delivers an annual freshwater input of about twice the total water volume of the entire Schlei (Gocke et al., 2003). Furthermore, spot #A is located ca. 100 m eastwards from the inflow of the small creek Mühlenbach (Figure 2a), and therefore susceptible to major freshwater discharge events. Likewise, the decreasing influence of freshwater inflow is clearly visible along the DZBC transect, with stronger impact on the seasonal salinity trends near the inflows of the river Recknitz (#B and #C) (Figures 2a and 5a). Short-term salinity fluctuations in the DZBC can be explained by influence of different water masses from either the eastern or western side of the ZS, which is controlled by wind direction and water level differences (Schumann et al., 2006).

By contrast, the areas close to the estuarine outflows towards the Baltic Sea are more susceptible to marine salinity dynamics. Those in turn are influenced by water intrusion events from the North Sea, via the Little Belt, Great Belt and Øresund (Mohrholz, 2018a, 2018b) (Figure 1). Especially in February 2020 large amounts of North Sea water was driven into the Baltic Sea (Mohrholz, 2018a, 2018b) (Figure 3), probably enforced by the same storms that contributed to enhanced precipitation amounts. These North Sea water masses are characterized by higher salinity and also by higher δ-values, compared with the Baltic Sea water (Harwood et al., 2008; Jefanova et al., 2020).

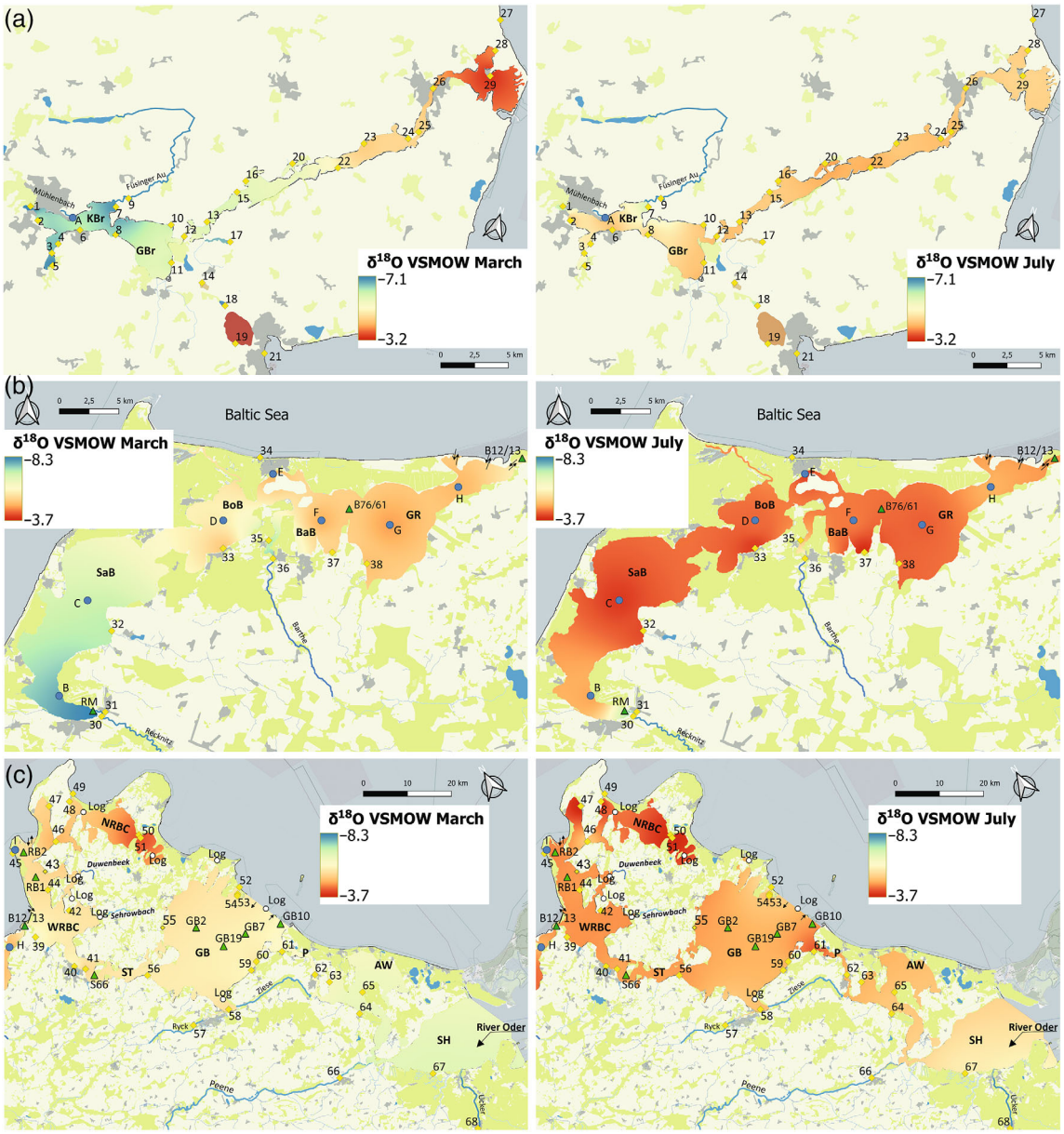

FIGURE 7 Interpolated $\delta^{18}O$ values along the three sampled transects for March (left) and July (right) 2020. Baltic Sea excluded from interpolation. Panels a–c refer to sub-regions as indicated in Figure 1. Circles #A–I: Sampling points for time series. Circles #1–68: Shore samples. Arrows indicate exchange points with Baltic Sea water. Abbreviations as in Figure 2.

The outermost Rügener Boddens (e.g. the WRBC including Vitter Bodden) are additionally shaped by complex dynamics within multiple influencing water masses: water is partially intruding from the Baltic Sea, south and northeast of Hiddensee island (Bachor, 2005). Freshwater surface runoff is derived from the NRBC (Hübel et al., 1998) (Figure 6). The boddens are further susceptible to large-scale water exchange with more eastern parts of the bodden coast, via the Strela Sound (Birr, 1988; Schiewer & Gocke, 1996).

In both the Vitter Bodden and the easternmost parts of the DZBC, salt water intrusion events from the North Sea (Figure 3) can explain the maximum salinities in February 2020 and 2021 (Figures 4–6). Strongly fluctuating values in February 2021 are probably influenced by the partial appearance and melting of an ice-cover across the boddens.

5.2 | Control mechanisms on water isotopes

All isotope time series exhibit strong seasonality of δ-values with comparable magnitude (ca. 2–3‰ $\delta^{18}O$; Figure 3–6). This suggests, that even the sampling points most distant from the freshwater inflows reflect a delayed and attenuated precipitation signal, that is a seasonality pattern as previously observed in German rivers (Reckerth et al., 2017) and northern German lakes (Aichner et al., 2022). Those

trends in δ^2H and δ^{18}O values are not fully mirrored by seasonal salinity changes, especially in the inner Schlei (#A), the outer Zingster boddens (#F–H) and the Vitter Bodden (#I) (Figures 3–6).

These results give evidence, that other factors than mixing processes between freshwater and marine water masses exhibit additional control on local water isotopes. We hypothesize, that ^{18}O/^{2}H-enrichment due to evaporation from surfaces of the shallow lagoons, such as the Kleine and Große Breite (Schlei) and the inner Zingster boddens, is a potential driver behind higher δ-values in summers. As estimated for the DZBC and the East Transect, the overall contribution of evaporation to the water budget is relatively low (<4%), while the largest contributors are riverine inflow and water exchange with the Baltic Sea (Chubarenko et al., 2005; Correns, 1977; Correns & Jäger, 1979; Lampe, 1994). On the other hand, potential evaporation exhibits a two to four times higher contribution to the overall water budget in the shallow inner lagoons of the DZBC (Saaler, Bodstedter and Barther Bodden), compared with the regions eastwards of the ZS (Grabow), and with the NRBC, the Stettiner Haff, and the Greifswalder Bodden (Lampe, 1994; Mertinkat, 1992). These spatial patterns, intermediated by morphometric factors such as shape and depths of the estuarine lagoon, might contribute to the seasonal isotope variability in these systems.

Furthermore, the correlations between water isotopes and water/air temperature, as well as O_2-saturation cannot rule out effects of these parameters onto δ-values. In winters, lower δ-values were observed in February/March 2021 compared with February/March 2020. This could indeed be explained by temperature control, due to the generally colder conditions with partially ice-cover on all sampling spots in winter/spring 2020/2021, compared with the relatively mild winter/spring 2019/2020 (reflected in water temperatures; Figures 3, 4 and 6).

In summer, the maximum δ-values are reached in September and early October (Figures 3, 4, and 6), that is 1–2 months delayed to maximum air and water temperatures. On the other hand, this timing is synchronous to maximum O_2-depletion (i.e. minimum O_2-concentration) at the sampling spot (Figures 3 and 4). The mechanistic relationship between phytoplankton blooms, local oxygen depletion and oversaturation, carbonate precipitation and pH values and their effects on oxygen isotopes in lacustrine waters have long been debated (e.g. Dietzel et al., 2009; Li et al., 2020; Quay et al., 1995). Likewise, an effect of this parameters on the measured δ^{18}O values cannot be fully excluded, but are considered as unlikely, because they do not explain synchronous trends in δ^2H values.

Near the estuarine outflows, the direct influence of Baltic Sea water onto the δ-values becomes apparent. Following the salt water intrusion events in February/March 2020, marine water with higher salinity and consequently higher δ-values shape the outflow environments of the estuaries. By contrast, lower salinities in July also lead to decreased δ-values in those realms (Figure 7).

We conclude, that specifically evaporation processes during summers are likely factors that lead to additional ^{18}O/^{2}H-enrichment on top of the seasonal signal as delivered by the riverine inflows. Other factors such as photosynthetic processes and related water chemical parameters are most likely of minor importance. Since the Baltic Sea is characterized by pronounced fluctuations in both salinity and isotope values, it shapes the water chemical conditions in its influence zone which include the outer estuarine regions.

5.3 | Salinity—Isotope correlation

The spatial trends in water isotopes as visualized in Figure 7 are illustrated as correlation crossplots between δ-values and salinities in Figure 8. Those reveal an almost linear correlation (R^2 0.99 δ^2H and 0.98 δ^{18}O; $p < 0.0001$) for samples taken along the Schlei in March 2020, and significant correlation (R^2 0.75 δ^2H and 0.77 δ^{18}O; $p < 0.0001$) for DZBC and Rügener Bodden samples. The isotope amplitude over ca. 20 salinity units accounted for ca. 30‰ δ^2H and 5.5‰ δ^{18}O.

By contrast, samples from July 2020 reveal hyperbolic correlations between the two parameters (Figure 8). Here, δ-values reach a plateau of maximum values for salinities >7. For some samples, a reversal towards lower δ-values with increasing salinities is observable. A similar trend is observable in samples from June 2019, which were taken in lower spatial resolution (Figure 8).

When analysing the three transects individually and in more detail, they all show a significant correlation between isotope values and salinity in March 2020 (Figure 9a). Especially in the Schlei, an almost linear correlation between δ-values and salinity is observable. Outliers with significant higher δ-values are samples taken from adjacent lakes and noors, which not or only weakly connected to the Schlei (Bültsee #14, Schnaaper See #18, Ornumer Noor #17 and Windebyer Noor #19) (Figure 7a). Furthermore, a sample from the close-by Baltic Sea location Eckernförde (#21) might be influenced by local mixing process different than in the Schlei system and its adjacent Baltic Sea outflow (e.g. #27, #29). In the DZBC, the March 2020 samples can be assigned to two clusters: (1) low saline samples taken from rivers or close to their outflows (#30/#31, #35/#36) and from Saaler Bodden (#32). (2) samples with salinity >6 psu from all other locations (Figures 7b and 9a). In the East Transect, again a linear salinity—isotope correlation is observed from the Stettiner Haff to Rügener Boddens, with one outlier (#51) derived from the inner NRBC (Figures 7c and 9a).

By contrast, in the Schlei and DZB, the two sampled summers (June 2019 and July 2020), reveal constant isotope values or even a reverse correlation from salinities 4 to 6 psu and higher on (Figure 9a). In the East Transect, however, a positive correlation along the Stettiner Haff—Peenestream—Greifswalder Bodden transect is observable, while samples from the WRBC, NRBC and adjacent Baltic Sea samples show mixed values clustering around −4.9 to −6.2‰ δ^{18}O and salinity values 8.1–9.6 psu (dashed black circles in Figure 9a,b).

These patterns come out more clearly when correlating δ-values to latitude/longitude, following their geographical orientations along the flow direction of the transects (Figure 9b), especially when considering the March–July offset of isotope values ($\Delta\delta$) (Figure 9c). This approach eliminates the influence of larger salinity ranges in March

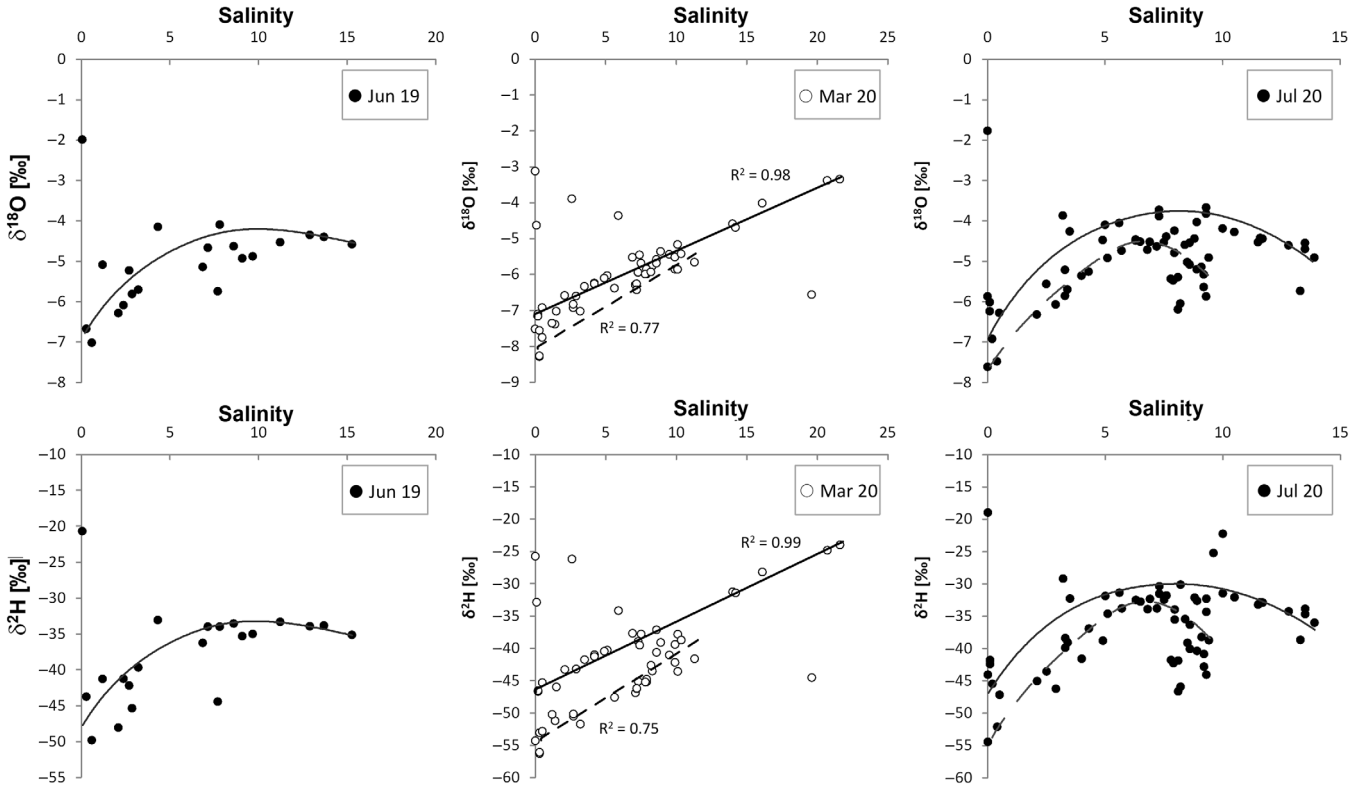

FIGURE 8 Correlation between $\delta^{18}O$ and $\delta^{2}H$ values and salinity in June 2019, March 2020, and July 2020. Linear and hyperbolic trendlines for Schlei (solid) and combined DZBC and Rügener Bodden (dashed) samples, under exclusion of outliers as derived from lakes and the open Baltic Sea.

compared with July, which is strongest in the Schlei, and makes isotope values from specific spots better comparable.

As noted above, most samples show isotope enrichment in the warmer season (i.e. negative $\Delta\delta$ March–July values) (Figure 7). Exceptions are a number of samples from the Baltic Sea, whose isotope signatures are rather driven by mixing processes than by seasonal trends, or samples under direct influence of Baltic Sea water (e.g. close to the outflows of the Schlei and DZBC). In general, samples show a tendency towards stronger isotope enrichment when located further inlands. Thus, they show increasing $\Delta\delta$ (March–July) values from the river inflows towards the Baltic Sea (Figure 9b,c; Figure 7; interpolated salinity and $\Delta\delta$ maps in Figure S1). Obviously, the shallow lagoons inlands (such as Kleine Breite at the Schlei, and Saaler and Bodstedter Boddens at DZBC) are more susceptible to undergo stronger isotopic enrichment in summers, than locations more adjacent to the Baltic Sea. This is most pronounced in the Schlei, here the $\Delta\delta$ values are balanced (i.e. similar isotope values in March and July) at ca. 75% of the distance between the inner Schlei and the outflow towards the Baltic Sea (Figure 9c). Beyond this place (which lies around the narrow passage aside the town Arnis, #24/#25), $\Delta\delta$ values become even positive due to lower δ-values in July compared with March (Figures 7a and Figure S1a).

The major inference from these data set is, that sampling points that undergo larger salinity changes between the maximum and minimum freshwater inflows in spring and summers (i.e. most negative ΔSal March–July) are also more susceptible to larger isotopic enrichment in the summers (more negative $\Delta\delta$ values March–July). This systematic is most pronounced in the Schlei, which is characterized by the most linear salinity gradient among the studied transects (Figure 9d). A similar trend is visible in the DZBC, but here it is weakened due to outliers as mainly derived from the Barther Bodden and Grabow samples. In the East Transect, no clear systematics between ΔSal and $\Delta\delta$ could be observed. While almost all samples show isotopic enrichment in summers (negative $\Delta\delta$), the stronger influence of mixing processes of multiple water sources (i.e. from rivers, inner Rügen boddens, Baltic Sea water intrusion from both the east and the north-west) can explain the heterogenous isotope values in this study area. Here, increasing sample density along sub-transects could potentially facilitate interpretation of isotope data and the control mechanisms behind.

6 | CONCLUSIONS

The results show that the studied estuarine systems exhibit a clear seasonality within their water isotope values. This is comparable to NE German lakes and rivers in both isotope amplitude and time succession. The data from three transects further reveal complex isotope versus salinity correlations: positive and significant correlations were observed in March 2020 along all transects. By contrast, hyperbolic

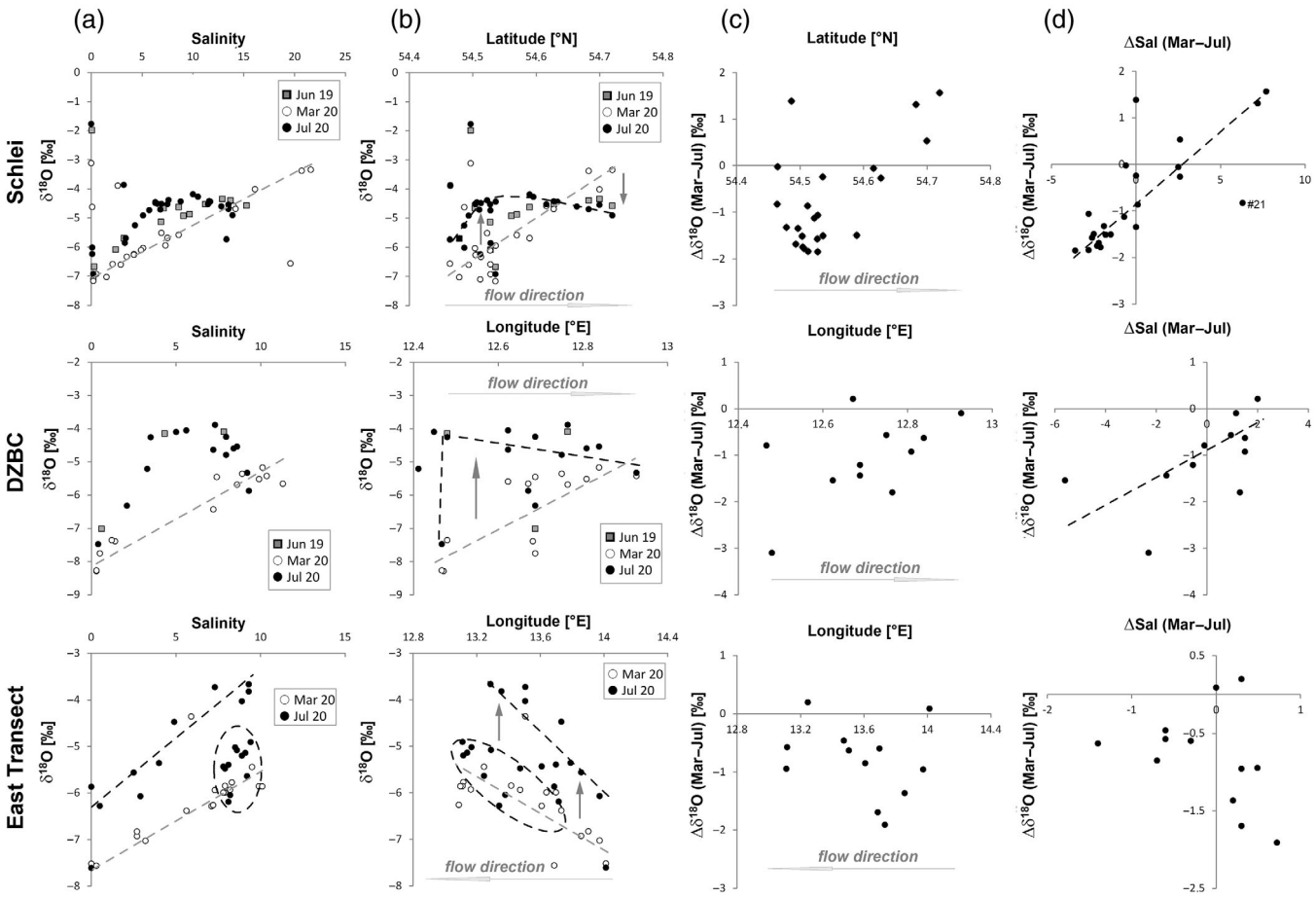

FIGURE 9 Correlations between: (a) $\delta^{18}O$ values and salinity. (b) $\delta^{18}O$ values and latitude or longitude. Dashed grey/black trendlines for March/July 2020. Vertical grey arrows indicate direction of isotopic change from March to July. Dashed black circle in the East Transect crossplots indicate Rügener Bodden and Baltic Sea samples. (c) $\Delta\delta^{18}O$ (March–July) and latitude or longitude. (d) $\Delta\delta^{18}O$ and ΔSal (March–July). DZBC: Darss-Zingst Bodden chain. East Transect comprises Stettiner Haff to GW Bodden and Rügener Boddens.

and partially inverse correlations were found in the two sampled summers (June 2019 and July 2020) along the Schlei and DZBC transects, while the spatially more extensive Eastern Transect still showed positive correlation.

We hypothesize that this is triggered by increased susceptibility of the shallow inland water basins to evaporative isotope enrichment in summers, causing higher δ-values. Furthermore, the discharge regime and isotope seasonality of tributary rivers is an important factor, with potentially a stronger impact near the inflows and the inner lagoons. In addition, the influence of water intrusion from the Baltic Sea can profoundly affect the water isotope signature of the outflow regions of the estuaries.

In summary, salinity is a fairly good predictor for water isotopes in winters, and on larger spatial scales in our study area. In summers and on regional scales, local hydrological processes are able to overprint the positive correlation between the two parameters, partly even leading to reverse correlations. This seasonality within the correlation of salinity versus water isotopes needs to be considered when interpreting biogenic isotope data (of plants or animals) because those might be similarly seasonally biased (often towards the warm/growing season).

ACKNOWLEDGEMENTS

Funding was provided by German Research Foundation (DFG) to B.A. (grant Ai 134/3-1). The authors are grateful to Volker Reiff, Henry Hansen and Jan Droll for help with sampling. The Wasserstraßen and Schifffahrtsamt Ostsee (WSA), the Staatliche Ämter für Landwirtschaft und Umwelt Vorpommern (STALU), the Landesamt für Landwirtschaft, Umwelt und ländliche Räume (LLUR), and the Bundesamt für Schifffahrt und Hydrographie (BSH) provided Baltic Sea water level, river discharge and evaporation data. The authors acknowledge two anonymous reviewers, whose constructive suggestions lead to improvement of the article. Open Access funding enabled and organized by Projekt DEAL.

DATA AVAILABILITY STATEMENT

The data that support the findings of this study are openly available in PANGAEA at https://doi.org/10.1594/PANGAEA.937990 (Aichner et al., 2021).

ORCID

Bernhard Aichner https://orcid.org/0000-0002-2471-7466

REFERENCES

Aichner, B., Dubbert, D., Dahlke, S., Duggen, S., Hansen, H., Rittweg, T., & Schumann, R. (2021). Water isotope values from estuarine systems along the German Baltic Sea coast. *PANGAEA*. https://doi.org/10.1594/PANGAEA.937990

Aichner, B., Dubbert, D., Kiel, C., Kohnert, K., Ogashawara, I., Jechow, A., Harpenslager, S.-F., Hölker, F., Nejstgaard, J. C., Grossart, H.-P., Singer, G., Wollrab, S., Berger, S. A., & Berger, S. A. (2022). Spatial and seasonal patterns of water isotopes in northeastern German lakes. *Earth System Science Data*, *2022*, 1857–1867. https://doi.org/10.5194/essd-14-1857-2022

Aichner, B., Hilt, S., Périllon, C., Gillefalk, M., & Sachse, D. (2017). Biosynthetic hydrogen isotopic fractionation factors during lipid synthesis in submerged aquatic macrophytes: Effect of groundwater discharge and salinity. *Organic Geochemistry*, *113*, 10–16.

Aichner, B., Makhmudov, Z. M., Rajabov, I., Zhang, Q., Pausata, F. S. R., Werner, M., Heinecke, L., Kuessner, M. L., Feakins, S. J., Sachse, D., & Mischke, S. (2019). Hydroclimate in the Pamirs was driven by changes in precipitation evaporation seasonality since the last glacial period. *Geophysical Research Letters*, *46*, 13972–13983.

Bachor, A. (2005). *Nährstoff- und Schwermetallbilanzen der Küstengewässer Mecklenburg-Vorpommerns unter besonderer Berücksichtigung ihrer Sedimente*. Landesamt für Umwelt, Naturschutz und Geologie.

Barrie, G. M., Worden, R. H., Barrie, C. D., & Boyce, A. J. (2015). Extensive evaporation in a modern temperate estuary: Stable isotopic and compositional evidence. *Limnology and Oceanography*, *60*(4), 1241–1250. https://doi.org/10.1002/lno.10091

Benetti, M., Reverdin, G., Aloisi, G., & Sveinbjornsdottir, A. (2017). Stable isotopes in surface waters of the Atlantic Ocean: Indicators of ocean-atmosphere water fluxes and oceanic mixing processes. *Journal of Geophysical Research-Oceans*, *122*(6), 4723–4742. https://doi.org/10.1002/2017jc012712

Birr, H.-D. (1988). Zu den Strömungsverhältnissen des Strelasundes. *Beiträge zur Meereskunde*, *58*, 3–8.

Birr, H.-D. (1997). Hydrographische Charakteristik und Umweltprobleme der mecklenburg-vorpommerschen Boddengewässer. *Greifswalder Geographische Arbeiten*, *14*, 111–128.

Bittar, T. B., Berger, S. A., Birsa, L. M., Walters, T. L., Thompson, M. E., Spencer, R. G. M., Mann, E. L., Stubbins, A., Frischer, M. E., & Brandes, J. A. (2016). Seasonal dynamics of dissolved, particulate and microbial components of a tidal saltmarsh-dominated estuary under contrasting levels of freshwater discharge. *Estuarine Coastal and Shelf Science*, *182*, 72–85. https://doi.org/10.1016/j.ecss.2016.08.046

Bowen, G. J., & Revenaugh, J. (2003). Interpolating the isotopic composition of modern meteoric precipitation. *Water Resources Research*, *39*(10), 1299. https://doi.org/10.1029/2003wr002086

Brennan, S. R., Cline, T. J., & Schindler, D. E. (2019). Quantifying habitat use of migratory fish across riverscapes using space-time isotope models. *Methods in Ecology and Evolution*, *10*(7), 1036–1047. https://doi.org/10.1111/2041-210x.13191

Chamberlayne, B. K., Tyler, J. J., & Gillanders, B. M. (2021). Controls over oxygen isotope fractionation in the waters and bivalves (*Arthritica helmsi*) of an estuarine lagoon system. *Geochemistry Geophysics Geosystems*, *22*(6), e2021GC009769. https://doi.org/10.1029/2021GC009769

Chubarenko, B., Chubarenko, I., & Baudler, H. (2005). Comparison of Darss-Zingst Bodden chain and Vistula Lagoon (Baltic Sea) in a view of hydrodynamic numerical modelling. *Baltica*, *18*(2), 56–67.

Correns, M. (1977). Grundzüge von Hydrographie und Wasserhaushalt der Boddengewässer an der Küste der Deutschen Demokratischen Republik. *Acta Hydrochimica et Hydrobiologica*, *5*, 517–526.

Correns, M., & Jäger, F. (1979). Beiträge zur Hydrographie der Nordrügenschen Bodden. I. Einführung in das Untersuchungsgebiet, Wasserstandsverhältnisse und Wasserhaushalt. *Acta Hydrophysica*, *23*, 149–177.

Craig, H. (1961). Isotopic variations in meteoric waters. *Science*, *133*(346), 1702–1703. https://doi.org/10.1126/science.133.3465.1702

Craig, H., & Gordon, L. I. (1965). *Deuterium and oxygen 18 variations in the ocean and marine atmosphere*. Proceedings of a conference on stable isotopes in oceanographic studies and palaeo temperatures. Spoleto, Italy, pp. 9–130.

Cyberski, J., Wróblewski, A., & Stewart, J. (2000). Riverine water inflows and the Baltic Sea water volume 1901–1990. *Hydrology and Earth System Sciences*, *4*(1), 1–11. https://doi.org/10.5194/hess-4-1-2000

Dansgaard, W. (1964). Stable isotopes in precipitation. *Tellus*, *16*(4), 436–468.

Dietzel, M., Tang, J., Leis, A., & Köhler, S. J. (2009). Oxygen isotopic fractionation during inorganic calcite precipitation—Effects of temperature, precipitation rate and pH. *Chemical Geology*, *268*(1), 107–115.

Dutton, A., Wilkinson, B. H., Welker, J. M., Bowen, G. J., & Lohmann, K. C. (2005). Spatial distribution and seasonal variation in O-18/O-16 of modern precipitation and river water across the conterminous USA. *Hydrological Processes*, *19*(20), 4121–4146. https://doi.org/10.1002/hyp.5876

Ehhalt, D. H. (1969). On the deuterium-salinity relationship in the Baltic Sea. *Tellus A*, *21*, 429–435.

Frew, R. D., Dennis, P. F., Heywood, K. J., Meredith, M. P., & Boswell, S. M. (2000). The oxygen isotope composition of water masses in the northern North Atlantic. *Deep-Sea Research Part I-Oceanographic Research Papers*, *47*(12), 2265–2286. https://doi.org/10.1016/S0967-0637(00)00023-6

Frohlich, K., Grabczak, J., & Rôwski, K. (1988). Deuterium and oxygen-18 in the Baltic Sea. *Chemical Geology: Isotope Geoscience Section*, *72*, 77–83.

Funkel, C. (2004). Jeschke, Lebrecht; Lenschow, Uwe; Zimmermann, Horst (Red.): Die Naturschutzgebiete in Mecklenburg-Vorpommern. *Naturschutz im Land Sachsen-Anhalt*, *41*(1), 60–62.

Gat, J. R., & Gonfiantini, R. (Eds.). (1981). *Stable isotope hydrology: Deuterium and Oxygen-18 in the water cycle* (Vol. 210). IAEA.

Gocke, K., Rheinheimer, G., & Schramm, W. (2003). Hydrographische, chemische und mikrobiologische Untersuchungen im Längsprofil der Schlei. *Schriften des Naturwissenschaftlichen Vereins für Schleswig-Holstein*, *68*, 31–62.

Grupe, G., Heinrich, D., & Peters, J. (2009). A brackish water aquatic foodweb: Trophic levels and salinity gradients in the Schlei fjord, Northern Germany, in Viking and medieval times. *Journal of Archaeological Science*, *36*, 2125–2144. https://doi.org/10.1016/j.jas.2009.05.011

Häggi, C., Chiessi, C. M., & Schefuß, E. (2015). Testing the D/H ratio of alkenones and palmitic acid as salinity proxies in the Amazon Plume. *Biogeosciences*, *12*, 7239–7249.

Halder, J., Terzer, S., Wassenaar, L. I., Araguas-Araguas, L. J., & Aggarwal, P. K. (2015). The global network of isotopes in rivers (GNIR): Integration of water isotopes in watershed observation and riverine research. *Hydrology and Earth System Sciences*, *19*(8), 3419–3431. https://doi.org/10.5194/hess-19-3419-2015

Harwood, A. J. P., Dennis, P. F., Marca, A., Pilling, G. M., & Millner, R. S. (2008). The oxygen isotope composition of water masses within the North Sea. *Estuarine Coastal and Shelf Science*, *78*, 353–359.

He, D., Nemiah Ladd, S., Saunders, C. J., Mead, R. N., & Jaffé, R. (2020). Distribution of *n*-alkanes and their δ^2H and δ^{13}C values in typical plants along a terrestrial-coastal-oceanic gradient. *Geochimica Et Cosmochimica Acta*, *281*, 31–52.

Hübel, H., & Dahlke, S. (1999). Die Nordrügenschen Boddengewässer-Entwicklung in Vergangenheit. Gegenwart und Zukunft. *Bodden*, *7*, 137–156.

Hübel, H., Wolff, C., & Meyer-Reil, L.-A. (1998). Salinity, inorganic nutrients, and primary production in a shallow coastal inlet in the southern Baltic Sea (Nordrügenschen Bodden) results from long-term

observations (1960–1989). *International Review of Hydrobiology*, *83*(5–6), 479–499. https://doi.org/10.1002/iroh.19980830516

Ingram, B. L., Conrad, M. E., & Ingle, J. C. (1996). Stable isotope and salinity systematics in estuarine waters and carbonates: San Francisco Bay. *Geochimica et Cosmochimica Acta*, *60*(3), 455–467. https://doi.org/10.1016/0016-7037(95)00398-3

Jasechko, S., Kirchner, J. W., Welker, J. M., & McDonnell, J. J. (2016). Substantial proportion of global streamflow less than three months old. *Nature Geoscience*, *9*(2), 126–129. https://doi.org/10.1038/ngeo2636

Jefanova, O., Mažeika, J., Petrošius, R., Skuratovič, Ž., Paškauskas, R., Martma, T., Liblik, T., & Ezhova, E. (2020). Baltic Sea water tritium and stable isotopes in 2016-2017. *Isotopes in Environmental and Health Studies*, *56*, 193–204.

Ladd, S. N., & Sachs, J. P. (2015). Hydrogen isotope response to changing salinity and rainfall in Australian mangroves. *Plant, Cell & Environment*, *38*(12), 2674–2687.

Ladd, S. N., & Sachs, J. P. (2017). $^{2}H/^{1}H$ fractionation in lipids of the mangrove Bruguiera gymnorhiza increases with salinity in marine lakes of Palau. *Geochimica et Cosmochimica Acta*, *204*, 300–312.

Lampe, R. (1994). Die vorpommerschen Boddengewässer—Hydrographie, Bodenablagerungen und Küstendynamik. In: *Die Küste 56* (pp. 25–49). Boyens.

Lampe, R. (1999). The Odra estuary as a filter and transformation area. *Acta Hydrochimica et Hydrobiologica*, *27*, 292–297.

Leduc, G., Sachs, J. P., Kawka, O. E., & Schneider, R. R. (2011). Holocene changes in eastern equatorial Atlantic salinity as estimated by water isotopologues. *Earth and Planetary Science Letters*, *362*, 151–162.

Li, H., Liu, X., Tripati, A., Feng, S., Elliott, B., Whicker, C., Arnold, A., & Kelley, A. M. (2020). Factors controlling the oxygen isotopic composition of lacustrine authigenic carbonates in Western China: Implications for paleoclimate reconstructions. *Scientific Reports*, *10*(1), 16370. https://doi.org/10.1038/s41598-020-73422-4

LLUR. (2001). *Ergebnisse langjähriger Wasseruntersuchungen in der Schlei. Eine Informations- und Planungsgrundlage*. Landesamt für Landwirtschaft, Umwelt und ländliche Räume Schleswig-Holstein.

LLUR. (2022). *Discharge data Füsinger Au 2019–2021*. Landesamt für Landwirtschaft, Umwelt und ländliche Räume Schleswig-Holstein. https://opendata.schleswig-holstein.de/dataset/abfluss-pegel-fusing-fusinger-au

Maloszewski, P., Rauert, W., Trimborn, P., Herrmann, A., & Rau, R. (1992). Isotope hydrological study of mean transit times in an Alpine Basin (Wimbachtal, Germany). *Journal of Hydrology*, *140*(1–4), 343–360. https://doi.org/10.1016/0022-1694(92)90247-S

Matta, M. E., Black, B. A., & Wilderbuer, T. K. (2010). Climate-driven synchrony in otolith growth-increment chronologies for three Bering Sea flatfish species. *Marine Ecology Progress Series*, *413*, 137–145. https://doi.org/10.3354/meps08689

McGuire, K. J., McDonnell, J. J., Weiler, M., Kendall, C., McGlynn, B. L., Welker, J. M., & Seibert, J. (2005). The role of topography on catchment-scale water residence time. *Water Resources Research*, *41*(5), W05002. https://doi.org/10.1029/2004wr003657

Meer, M. T. J., Baas, M., Rijpstra, W. I. C., Marino, G., Rohling, E. J., Damsté, J. S. S., & Schouten, S. (2007). Hydrogen isotopic compositions of long-chain alkenones record freshwater flooding of the Eastern Mediterranean at the onset of sapropel deposition. *Earth and Planetary Science Letters*, *262*, 594–600.

Mertinkat, L. (1992). *Wasserhaushaltsdaten der Bodden- und Haffgewässer*. Unveröff. Mitt. Bundesamt für Seeschiffahrt und Hydrographie.

Mohan, J. A., & Walther, B. D. (2015). Spatiotemporal variation of trace elements and stable isotopes in subtropical estuaries: II. Regional, local, and seasonal salinity-element relationships. *Estuaries and Coasts*, *38*(3), 769–781. https://doi.org/10.1007/s12237-014-9876-4

Mohrholz, V. (2018a). *Baltic saline barotropic inflows (SBI) 1887–2018*. dataset 2019–2021. https://doi.org/10.12754/data-2018-0004

Mohrholz, V. (2018b). Major Baltic inflow statistics—revised. *Frontiers in Marine Science*, *5*, 384. https://doi.org/10.3389/fmars.2018.00384

Ogrinc, N., Kanduc, T., Stichler, W., & Vreca, P. (2008). Spatial and seasonal variations in delta O-18 and delta D values in the River Sava in Slovenia. *Journal of Hydrology*, *359*(3–4), 303–312. https://doi.org/10.1016/j.jhydrol.2008.07.010

Orlowski, N., Kraft, P., Pferdmenges, J., & Breuer, L. (2016). Exploring water cycle dynamics by sampling multiple stable water isotope pools in a developed landscape in Germany. *Hydrology and Earth System Sciences*, *20*(9), 3873–3894. https://doi.org/10.5194/hess-20-3873-2016

Patterson, W. P., Smith, G. R., & Lohmann, K. C. (1993). Continental paleothermometry and seasonality using the isotopic composition of aragonitic otoliths of freshwater fishes. *GMS*, *78*, 191–202.

Price, R. M., Skrzypek, G., Grierson, P. F., Swart, P. K., & Fourqurean, J. W. (2012). The use of stable isotopes of oxygen and hydrogen to identify water sources in two hypersaline estuaries with different hydrologic regimes. *Marine and Freshwater Research*, *63*(11), 952–966. https://doi.org/10.1071/Mf12042

Quay, P. D., Wilbur, D., Richey, J. E., Devol, A. H., Benner, R., & Forsberg, B. R. (1995). The 18O:16O of dissolved oxygen in rivers and lakes in the Amazon Basin: Determining the ratio of respiration to photosynthesis rates in freshwaters. *Limnology and Oceanography*, *40*(4), 718–729. https://doi.org/10.4319/lo.1995.40.4.0718

Reckerth, A., Stichler, W., Schmidt, A., & Stumpp, C. (2017). Long-term data set analysis of stable isotopic composition in German rivers. *Journal of Hydrology*, *552*, 718–731. https://doi.org/10.1016/j.jhydrol.2017.07.022

Richter, W. V., & Kowski, P. (1990). Deuterium and Oxygen-18 in surface waters of GDR draining to the Baltic Sea. *Isotopes in Environmental and Health Studies*, *26*, 569–573.

Rodgers, P., Soulsby, C., Waldron, S., & Tetzlaff, D. (2005). Using stable isotope tracers to assess hydrological flow paths, residence times and landscape influences in a nested mesoscale catchment. *Hydrology and Earth System Sciences*, *9*(3), 139–155. https://doi.org/10.5194/hess-9-139-2005

Sachs, J. P., & Schwab, V. F. (2011). Hydrogen isotopes in dinosterol from the Chesapeake Bay estuary. *Geochimica et Cosmochimica Acta*, *75*, 444–459.

Schiewer, U. (2008). *Ecology of Baltic coastal waters. Ecological studies* (Vol. 147). Springer.

Schiewer, U., & Gocke, K. (1996). Ökologie der Bodden und Förden. In G. Rheinheimer (Ed.), *Meereskunde der Ostsee* (pp. 216–221). Springer.

Schouten, S., Ossebaar, J., Schreiber, K., Kienhuis, M. V. M., Langer, G., Benthien, A., & Bijma, J. (2006). The effect of temperature, salinity and growth rate on the stable hydrogen isotopic composition of long chain alkenones produced by *Emiliania huxleyi* and *Gephyrocapsa oceanica*. *Biogeosciences*, *3*, 113–119.

Schulz, H. (1979). Ein numerisches Modell des Wasserhaushalts und der Wasserbeschaffenheit in der Ostseebucht Schlei. *Senckenbergiana Maritima*, *11*, 175–192.

Schumann, R., Baudler, H., Glass, Ä., Dümcke, K., & Karsten, U. (2006). Long-term observations on salinity dynamics in a tideless shallow coastal lagoon of the Southern Baltic Sea coast and their biological relevance. *Journal of Marine Systems*, *60*, 330–344.

Schwarzer, K., Ricklefs, K., Bartholomä, A., & Zeiler, M. (2008). Geological development of the North Sea and the Baltic Sea. *Die Küste*, *74*, 1–17.

Seiß, G. (2014). *Impact of sea level change on inner coastal waters of the Baltic Sea*. Bundesanstalt für Wasserbau.

Sklash, M. G., Farvolden, R. N., & Fritz, P. (1976). Conceptual-model of watershed response to rainfall, developed through use of Oxygen-18 as a natural tracer. *Canadian Journal of Earth Sciences*, *13*(2), 271–283. https://doi.org/10.1139/e76-029

STALU. (2022). *Discharge rates of Mecklenburg-Vorpommern rivers 2019–2021*. Staatliche Ämter für Landwirtschaft und Umwelt Mecklenburg-Vorpommern.

Swart, P. K., & Price, R. (2002). Origin of salinity variations in Florida Bay. *Limnology and Oceanography*, *47*(4), 1234–1241. https://doi.org/10.4319/lo.2002.47.4.1234

Torniainen, J., Lensu, A., Vuorinen, P. J., Sonninen, E., Keinänen, M., Jones, R. I., Patterson, W. P., & Kiljunen, M. (2017). Oxygen and carbon isoscapes for the Baltic Sea: Testing their applicability in fish migration studies. *Ecology and Evolution*, *7*, 2255–2267.

Trueman, C. N., Mackenzie, K. M., & Palmer, M. R. (2012). Identifying migrations in marine fishes through stable-isotope analysis. *Journal of Fish Biology*, *81*(2), 826–847. https://doi.org/10.1111/j.1095-8649.2012.03361.x

WSA-WSV. (2022). *Baltic Sea water level data 2019-2021*. Wasserstraßen and Schifffahrtsamt Ostsee. In der: Wasserstraßen und Schifffahrtsverwaltung des Bundes (WSV). Lübeck.

Zanden, H. B. V., Soto, D. X., Bowen, G. J., & Hobson, K. A. (2016). Expanding the isotopic toolbox: Applications of hydrogen and oxygen stable isotope ratios to food web studies. *Frontiers in Ecology and Evolution*, *4*. https://doi.org/10.3389/fevo.2016.00020

SUPPORTING INFORMATION

Additional supporting information can be found online in the Supporting Information section at the end of this article.

How to cite this article: Aichner, B., Rittweg, T., Schumann, R., Dahlke, S., Duggen, S., & Dubbert, D. (2022). Spatial and temporal dynamics of water isotopes in the riverine-marine mixing zone along the German Baltic Sea coast. *Hydrological Processes*, *36*(9), e14686. https://doi.org/10.1002/hyp.14686